

Transition of laser cooling between standard and Raman optical lattices

R. Zhang, R. E. Sapiro, N. V. Morrow, and G. Raithel

FOCUS Center, Department of Physics, University of Michigan, Ann Arbor, Michigan, 48109–1040 USA

(Received 9 June 2006; published 13 September 2006)

Reduced-period optical lattices based on Raman transitions allow for sub-Doppler laser cooling. An important parameter of this Raman optical lattice is the frequency difference Δ_d between two virtual energy levels involved in the atom-field interaction scheme. In this work, we use experimental time-of-flight data and quantum simulations to characterize laser cooling in the Raman lattice as a function of Δ_d . Two different domains of laser cooling are identified. For small Δ_d , atoms are cooled due to a well-known mechanism that also occurs in standard optical lattices. For large Δ_d , atoms are cooled based on Raman transitions. We study the transition between the two domains of laser cooling in detail.

DOI: [10.1103/PhysRevA.74.033404](https://doi.org/10.1103/PhysRevA.74.033404)

PACS number(s): 32.80.Pj, 33.80.Wz

Optical lattices, formed by the interference of multiple laser beams, generate light-shift potentials that are employed widely to trap and manipulate laser-cooled atoms [1,2]. Employing different atomic transitions, lattice-beam geometries, intensities, and frequencies, a large variety of optical lattices can be formed [3], leading to many applications in fundamental and applied physics. Optical lattices have been used to study transient one-body quantum phenomena, such as Landau-Zener tunneling [4], Bloch oscillations [5], Wannier-Stark states [6], wave-packet revivals [7], and tunneling [8,9]. Optical lattices have applications in atom lithography, as reviewed in Refs. [2,10], and in quantum information processing [11,12]. The dynamics of many-body quantum gases in optical lattices has become an active research field and has recently been reviewed [13].

There is an interest in optical lattices with spatial periods less than the periodicity of a basic one-dimensional standing wave (which is $\lambda/2$, where λ is the laser wavelength). Laser cooling and atom localization in such reduced-period optical lattices could be applied in nanolithography, where the deposition of regular patterns with reduced spatial periods is desirable. Reduced-period lattices could also be used to prepare spatially periodic quantum gases with densities higher than those achievable in basic optical lattices. Structures as small as $\lambda/8$ have been created using multiple optical potentials [14]. This paper deals with a more general, scalable approach to reduce the lattice periodicity, relying on the use of Raman transitions [15–18]. Here, the lattice periodicity is given by $\lambda/(2N)$, where N is the order of the employed Raman transition. Recently, we demonstrated sub-Doppler laser cooling in a one-dimensional Raman optical lattice (ROL), both theoretically [19] and experimentally [20]. In our experiments, four lattice beams with different frequencies drive the $5S_{1/2}, F=1 \rightarrow 5P_{3/2}, F'=1$ transition of ^{87}Rb atoms ($\lambda = 780$ nm), as indicated in Fig. 1. The lattice beams are blue-detuned from the atomic transition by an amount Δ of several line-widths Γ ($\Gamma/2\pi = 6$ MHz). The combination of field 1 (σ^+ -polarized) and field 2 (σ^- -polarized) drives two-photon Raman transitions between the magnetic sublevels $|m=1\rangle$ and $|m=-1\rangle$ of the ground state. Since the atom-field detuning Δ is much larger than Γ and the relevant single-photon Rabi frequencies, the excited state $5P_{3/2}, F'=1$ becomes only weakly populated; in the theoretical analysis, the excited

state can be adiabatically eliminated. As a result, the coupling between the $|m=1\rangle$ and $|m=-1\rangle$ sublevels of the ground state can be considered as arising from an effective Raman field with wave vector $2k_L\hat{z}$, where $k_L = 2\pi/\lambda$. The ROL incorporates two additional fields, 3 and 4, that counterpropagate with fields 1 and 2 (see Fig. 1). Fields 3 and 4 result in an effective Raman field with wave vector $-2k_L\hat{z}$. The two Raman fields interfere, leading to a modulation of the ground-state populations and coherences that vary as $\cos(4k_L z)$.

In order to obtain the cooling and atom-localization effects in the lattice formed by the two counterpropagating Raman fields (which drive two-photon transitions), perturbations caused by interference of counterpropagating pairs of the fundamental traveling-wave fields (which drive single-photon transitions) must be suppressed. This suppression is achieved by choosing sufficiently different atom-field detunings Δ for field pair 1 and 2 and pair 3 and 4. The respective detunings will henceforth be referred to as Δ_1 and Δ_2 , and the difference will be denoted $\Delta_d = |\Delta_2 - \Delta_1|$ (see Fig. 1). In our previous work [19,20], Δ_d was set equal to 4 MHz, which was large enough that all interference effects caused by counterpropagating pairs of traveling-wave fields in the system were negligible. In the present work, we systematically reduce the value of Δ_d to zero and examine the breakdown of ROL laser cooling that occurs as a result of the gradual onset of perturbations caused by the interference of one-photon fields. Conditions on the minimal value of Δ_d are obtained for which sub-Doppler cooling in the ROL is effective. It is further seen that, as Δ_d approaches zero, the system

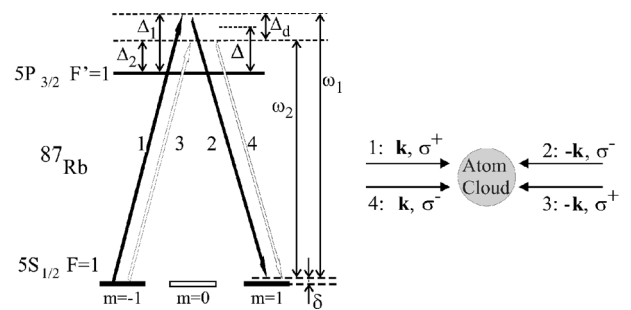


FIG. 1. Level scheme and atom-field detunings (left), field directions and polarizations (right).

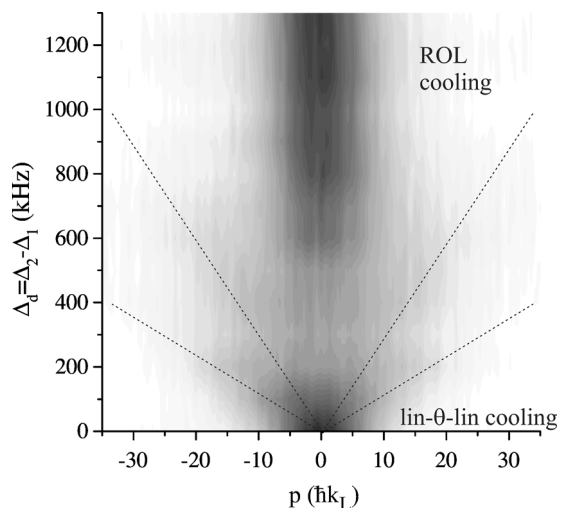


FIG. 2. Momentum distributions of atoms, obtained from experimental time-of-flight data, as a function of Δ_d . The average lattice detuning Δ is 5Γ , and the single-beam lattice intensity is 2 mW/cm^2 . The atoms are cooled for $150 \mu\text{s}$ in the lattice. The figure shows two domains of efficient laser cooling, namely, $\Delta_d \leq 100 \text{ kHz}$ and $\Delta_d \geq 600 \text{ kHz}$, as well as a regular pattern identified by the dotted lines.

approaches a well-known two-field configuration that yields sub-Doppler Sisyphus cooling, namely, the case of two counterpropagating fields with linear polarizations that form an angle θ (“lin- θ -lin”-cooling; see Refs. [21,22]).

In the experiment, Rb atoms are collected and precooled to $\sim 50 \mu\text{K}$ using a magneto-optic trap (MOT) and a six-beam corkscrew optical molasses. The atoms are then further cooled in a ROL with beam directions and polarizations as shown in Fig. 1. The ROL cooling occurs under magnetic-field-free conditions and lasts $150 \mu\text{s}$. The four ROL lattice beams are derived from a single laser source, which is stabilized to within 1 MHz. The frequencies of individual beams are shifted by acousto-optic modulators (AOM), which are driven by stable RF generators. Beams 1 and 2 have frequency ω_1 ; beams 3 and 4 have frequency ω_2 (in most cases, $\omega_1 \neq \omega_2$; see Fig. 1). Since the magnetic field is zero to within a few microgauss, the magnetic sublevels are quasi-degenerate, and beam pairs 1+2 and 3+4 are quasi-resonant with the Raman transition connecting the ground-state sublevels $|m=1\rangle$ and $|m=-1\rangle$. In this way, the detuning difference $\Delta_d = |\Delta_2 - \Delta_1|$ is fixed to within a kilohertz and the Raman detuning δ in Fig. 1 is maintained at zero, with a variation of less than about 5 kHz. Provided that Δ_d is sufficiently large, these conditions yield the best sub-Doppler cooling in the ROL [20]. We study the transition from laser cooling in a lin- θ -lin lattice to laser cooling in the ROL as a function of Δ_d , which is varied by changing the frequencies of the RF generators that drive the AOMs.

We use a standard time-of-flight (TOF) technique to measure the momentum distributions after $150 \mu\text{s}$ of laser cooling in the lattice. Under each condition, 30 TOF signals are collected and averaged using an oscilloscope. The detuning difference Δ_d is varied in steps of 100 kHz. In Fig. 2, experimental momentum distributions obtained for a typical lattice intensity and detuning and for different values of Δ_d are dis-

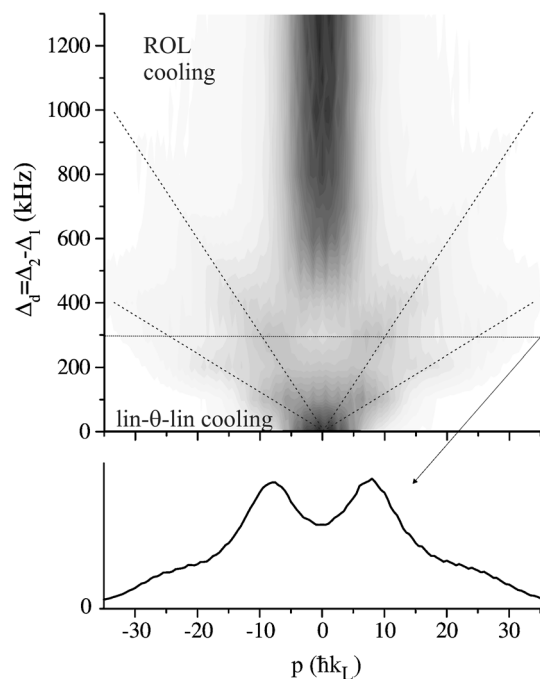


FIG. 3. Top panel: Simulated momentum distribution of atoms as a function of Δ_d after $150 \mu\text{s}$ ROL cooling. The average detuning is 5Γ , and the single-beam lattice intensity is 2 mW/cm^2 . The simulation agrees well with experimental data displayed in Fig. 2. Bottom panel: Momentum distribution at $\Delta_d = 300 \text{ kHz}$.

played in a two-dimensional grayscale representation. We observe efficient sub-Doppler cooling for $\Delta_d \leq 100 \text{ kHz}$. In a range $200 \text{ kHz} \leq \Delta_d \leq 500 \text{ kHz}$, no cooling effect is observed; however, in that domain the momentum distributions appear to be modulated by a regular pattern (see dotted lines in Figs. 2 and 3). Over a range $500 \text{ kHz} \leq \Delta_d \leq 800 \text{ kHz}$ sub-Doppler cooling redevelops and reaches a steady level for $\Delta_d \geq 800 \text{ kHz}$.

The cooling dynamics are also simulated using the quantum Monte-Carlo wave-function method (QMCWF), which was introduced in Ref. [23] and has frequently been used to model laser cooling [24]. The simulations employ a fully quantum-mechanical description of the internal and center-of-mass degrees of freedom of the atoms. The QMCWF allows us to determine the spatial and momentum distributions of the atoms, including the degree to which the atoms become localized in the wells of the lattice potentials. As seen in Fig. 3, the QMCWF simulations reproduce the experimentally observed cooling behavior well.

The physics of the cooling can be qualitatively explained as follows. The copropagating, spatially overlapping σ^+ and σ^- lattice beams 1 and 4 are equivalent to a single, linearly polarized net field, the polarization plane of which rotates at a frequency $\Delta_d/2$. Beams 2 and 3 are equivalent to an analogous net field. In a fixed, beam-independent frame, the polarization planes of the net fields rotate in opposite directions. If the rotation period $2/\Delta_d$ is of order of or exceeds the time it takes for an atom to lasercool in a two-beam lin- θ -lin lattice, the cooling behavior is expected to be similar to that of the lin- θ -lin lattice [21,22]. For the conditions in Fig. 2, we have found that for the case $\Delta_d = 0$ the time required to

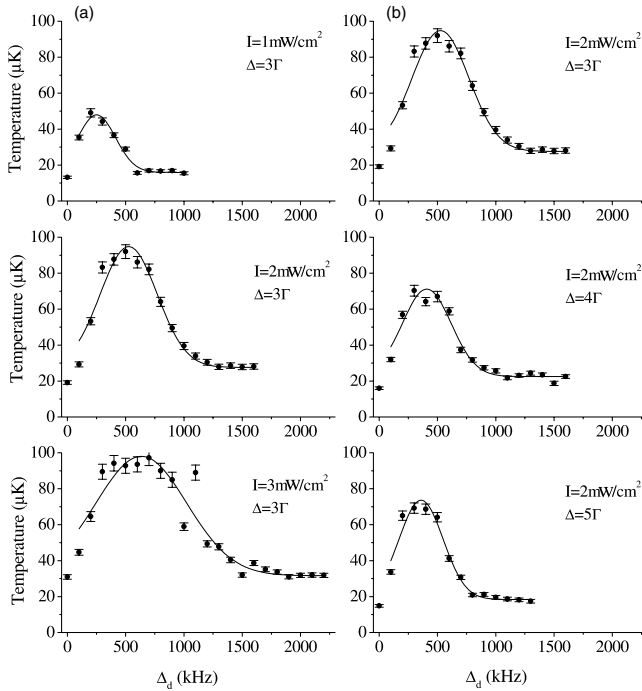


FIG. 4. Temperature of the atoms as a function of Δ_d for different (a) lattice beam intensities and (b) average atom-field detunings. The lines show Gaussian fits to the data.

cool the atoms is of order $50 \mu\text{s}$. This suggests that lin- θ -lin cooling should be effective for detuning differences $\Delta_d \lesssim 50 \text{ kHz}$. In agreement with this very simple estimate, we find experimentally that the lin- θ -lin cooling is effective for $\Delta_d \lesssim 100 \text{ kHz}$.

The singular case $\Delta_d=0$ corresponds to well-known Sisyphus cooling in a stationary lin- θ -lin lattice [21,22]. In the experiment, the value of θ varies from one repetition of the lattice cooling to the next due to phase variations in the lattice beams caused by thermal and mechanical instabilities and air turbulence. Since the cooling data are typically collected over a period of order 1 min, we assume that the data for $\Delta_d=0$ represent an average for a uniform probability distribution in θ . During any given repetition of the cooling, the phase θ is approximately constant. We have seen in the QM-CWF simulations that the cooling efficiency and speed do not vary much over a range $\pi/16 \leq \theta \leq \pi/2$, whereas in the range $0 \leq \theta \leq \pi/16$ the cooling is slow and the steady-state temperature is of order twice the θ -averaged temperature. These findings explain another experimental observation: in the case $\Delta_d=0$, the cooling works well in most individual repetitions; in about one out of ten repetitions, it apparently fails.

In the range $200 \text{ kHz} \leq \Delta_d \leq 500 \text{ kHz}$, the angle between the linear polarizations of the counterpropagating lattice beams rotates too fast for lin- θ -lin cooling to be effective. Also, Δ_d is not large enough for the sub-Doppler cooling mechanism of the ROL (described in detail [21,22]) to be effective. As a result, in this range no significant cooling occurs. There is, however, some cooling into frames of reference moving at velocities of $v = \pm \lambda \Delta_d / 2$ and $v = \pm \lambda \Delta_d / 4$, identified by the dotted lines in Figs. 2 and 3. The accumu-

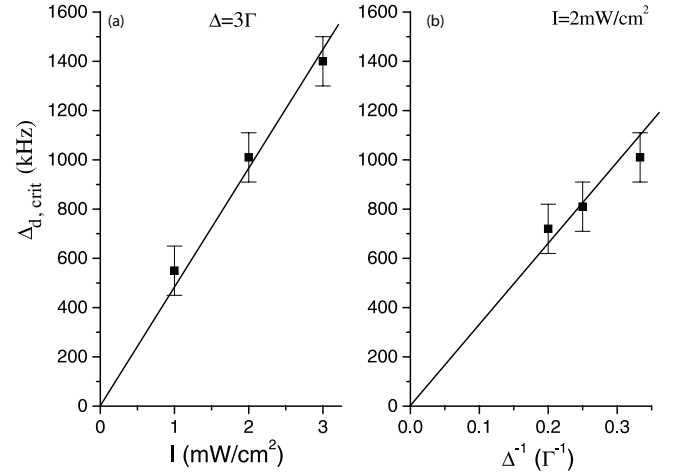


FIG. 5. Critical detuning difference $\Delta_{d,\text{crit}}$ beyond which the sub-Doppler cooling in the ROL occurs (a) vs the lattice-beam intensity I at fixed average detuning Δ and (b) vs Δ^{-1} at fixed I .

lation of atoms at these velocities is most clearly seen in the substructures in the bottom panel of Fig. 3.

The case $v = \pm \lambda \Delta_d / 2$ can be interpreted as a cooling type similar to magnetic-field-induced laser cooling (MILC) [25], in which atoms are cooled into σ^+ - or σ^- -standing waves. For instance, the σ^+ -standing wave generated by beams 1 and 3 of Fig. 1 moves at a velocity of $v = \lambda \Delta_d / 2$. The atoms cooled into the light-shift potentials associated with that standing wave move at an average velocity of $\lambda \Delta_d / 2$. To obtain Sisyphus-type laser cooling, some mixing is required between the states associated with the light-shift potentials generated by the moving σ^+ -standing wave. In MILC, the mixing is provided by a weak transverse magnetic field [25]. In the present case, the mixing is provided by Raman couplings involving pairs of σ^+ and σ^- beams in Fig. 1.

The case $v = \pm \lambda \Delta_d / 4$ may result from atom-field interactions involving three of the four beams in Fig. 1. For instance, in a reference frame moving at a velocity $v = \lambda \Delta_d / 4$ the beams 1, 2, and 3 generate an atom-field interaction involving two fields of the same frequency, namely, a σ^+ wave with wave-vector $+\mathbf{k}$, and a linearly polarized wave with wave vector $-\mathbf{k}$ whose polarization rotates slowly with a frequency of $\Delta_d / 2$. This combination of fields produces some sub-Doppler cooling.

We quantitatively characterize the dependence of the temperature on Δ_d for different atom-field detunings Δ and lattice-beam intensities I . For each set (Δ, I) , the momentum distribution obtained from measured, averaged TOF signals is fit by a Gaussian distribution with momentum standard deviation σ_p . The temperature of the atoms is $T = \frac{\sigma_p^2}{M k_B}$, where M is the atomic mass and k_B the Boltzmann constant. The resulting temperatures versus Δ_d are shown in Fig. 4. In the series displayed in Fig. 4(a), the parameter Δ is kept fixed and the intensity I is varied, while in 4(b) I is kept fixed and Δ is varied.

In all data sets in Fig. 4, for values of Δ_d close to zero, the temperature rapidly increases with Δ_d . This behavior is attributed to the breakdown of Sisyphus cooling in the lin- θ -lin lattice geometry. There is a wide range of Δ_d with no cool-

ing. For Δ_d larger than certain critical values, $\Delta_{d,\text{crit}}$, ROL sub-Doppler cooling occurs. In the limit of large Δ_d , the temperature in the ROL converges toward a temperature slightly higher than that obtained in the lin- θ -lin lattice for $\Delta_d=0$. All these observations have been reproduced using QMCWF simulations.

As shown in Fig. 4, the data sets are fit quite well by Gaussians with offsets. The Gaussians are centered at values Δ_0 and have standard deviations σ_Δ . We define the critical detuning-difference beyond which ROL cooling occurs as $\Delta_{d,\text{crit}}=\Delta_0+\sigma_\Delta$. It is apparent that with increasing lattice beam intensity I , the values of $\Delta_{d,\text{crit}}$ increase, whereas for increasing average detuning Δ , they decrease. To exhibit these trends more clearly, in Fig. 5 we plot $\Delta_{d,\text{crit}}$ vs intensity I and detuning Δ^{-1} . The experimental evidence suggests that $\Delta_{d,\text{crit}}$ is proportional to both the lattice beam intensity I and to Δ^{-1} .

The observed scaling of $\Delta_{d,\text{crit}}$ can be qualitatively explained by the basic assumptions made in the theoretical treatment of the ROL [19]. These assumptions are that the value of Δ_d is sufficiently large to ensure that fields 1 and 3 (or 2 and 4) do not interfere while they drive *single* photon transitions, and that fields 1 and 4 (or 2 and 3) do not drive Raman transitions. The light shifts due to the traveling-wave

fields and the coupling strength of the Raman transitions are both characterized by $\frac{\chi^2}{\Delta}$, where $\chi=-\frac{\mu E}{2\hbar}$ is the Rabi frequency [19]. We expect that the above assumptions are satisfied when Δ_d is larger than a value $\propto \frac{\chi^2}{\Delta} \propto \frac{I}{\Delta}$. This expectation is in accordance with the experimentally observed Δ_d dependence.

In summary, we have investigated the transition between standard “lin- θ -lin” laser cooling and laser cooling due to Raman transitions in a one-dimensional Raman optical lattice. Experimental results are in good agreement with quantum simulations. In the future, Raman lattices may have applications in atom lithography and in cold-atom manipulation in cases where reduced-period structures are desired. In ongoing work, we intend to experimentally verify the $\lambda/4$ periodicity of the ROL using optical-mask techniques [26]. An extension of the ROL scheme to higher-order Raman transitions, which are expected to yield even smaller lattice periods, will also be pursued.

We thank Paul Berman for inspiring discussions. The research has been supported by National Science Foundation under Grants No. PHY-0555520 and No. FOCUS (PHY-0114336).

-
- [1] P. S. Jessen and I. H. Deutsch, *Adv. At., Mol., Opt. Phys.* **37**, 95 (1996).
 - [2] G. Grynberg and C. Robilliard, *Phys. Rep.* **355**, 335 (2001).
 - [3] K. I. Petsas, A. B. Coates, and G. Grynberg, *Phys. Rev. A* **50**, 5173 (1994).
 - [4] Q. Niu, X.-G. Zhao, G. A. Georgakis, and M. G. Raizen, *Phys. Rev. Lett.* **76**, 4504 (1996).
 - [5] M. Ben Dahan, E. Peik, J. Reichel, Y. Castin, and C. Salomon, *Phys. Rev. Lett.* **76**, 4508 (1996).
 - [6] S. R. Wilkinson, C. F. Bharucha, K. W. Madison, Q. Niu, and M. G. Raizen, *Phys. Rev. Lett.* **76**, 4512 (1996).
 - [7] G. Raithel, W. D. Phillips, and S. L. Rolston, *Phys. Rev. Lett.* **81**, 3615 (1998).
 - [8] S. K. Dutta, B. K. Teo, and G. Raithel, *Phys. Rev. Lett.* **83**, 1934 (1999).
 - [9] D. L. Haycock, P. M. Alsing, I. H. Deutsch, J. Grondalski, and P. S. Jessen, *Phys. Rev. Lett.* **85**, 3365 (2000).
 - [10] C. Bradley, W. Anderson, J. McClelland, and R. Celotta, *Appl. Surf. Sci.* **141**, 210 (1999).
 - [11] G. K. Brennen, C. M. Caves, P. S. Jessen, and I. H. Deutsch, *Phys. Rev. Lett.* **82**, 1060 (1999).
 - [12] D. Jaksch, H.-J. Briegel, J. I. Cirac, C. W. Gardiner, and P. Zoller, *Phys. Rev. Lett.* **82**, 1975 (1999).
 - [13] I. Bloch, *Phys. World*, **17** (4), 25 (2004).
 - [14] R. Gupta, J. J. McClelland, P. Marte, and R. J. Celotta, *Phys. Rev. Lett.* **76**, 4689 (1996).
 - [15] P. R. Berman, B. Dubetsky, and J. L. Cohen, *Phys. Rev. A* **58**, 4801 (1998).
 - [16] B. Dubetsky and P. R. Berman, *Laser Phys.* **12**, 1161 (2002).
 - [17] B. Dubetsky and P. R. Berman, *Phys. Rev. A* **66**, 045402 (2002).
 - [18] M. Weitz, G. Cennini, G. Ritt, and C. Geckeler, *Phys. Rev. A* **70**, 043414 (2004).
 - [19] P. R. Berman, G. Raithel, R. Zhang, and V. S. Malinovsky, *Phys. Rev. A* **72**, 033415 (2005).
 - [20] R. Zhang, N. V. Morrow, P. R. Berman, and G. Raithel, *Phys. Rev. A* **72**, 043409 (2005).
 - [21] V. Finkelstein, P. R. Berman, and J. Guo, *Phys. Rev. A* **45**, 1829 (1992).
 - [22] J. Guo and P. R. Berman, *Phys. Rev. A* **48**, 3225 (1993).
 - [23] J. Dalibard, Y. Castin, and K. Molmer, *Phys. Rev. Lett.* **68**, 580 (1992).
 - [24] P. Marte, R. Dum, R. Taieb, and P. Zoller, *Phys. Rev. A* **47**, 1378 (1993).
 - [25] B. Sheehy, S.-Q. Shang, P. van der Straten, S. Hatamian, and H. Metcalf, *Phys. Rev. Lett.* **64**, 858 (1990).
 - [26] A. Turlapov, A. Tonyushkin, and T. Sleator, *Phys. Rev. A* **68**, 023408 (2003).